ACS APPLIED MATERIALS & INTERFACES

Research Article

Cite This: ACS Appl. Mater. Interfaces 2019, 11, 10118−10127

www.acsami.org

Facile Preparation of Cu/Ag Core/Shell Electrospun Nanofibers as Highly Stable and Flexible Transparent Conductive Electrodes for Optoelectronic Devices

Dai-Hua Jiang,[†,‡,§,#] Ping-Chun Tsai,[†,#] Chi-Ching Kuo,[*,†,∥] Fu-Cheng Jhuang,[†] Hao-Cheng Guo,[†] Shih-Pin Chen,[⊥] Ying-Chih Liao,[⊥] Toshifumi Satoh,[*,§] and Shih-Huang Tung[*,‡]

[†]Institute of Organic and Polymeric Materials and [∥]Research and Development Center for Smart Textile Technology, National Taipei University of Technology, Taipei 10608, Taiwan

[‡]Institute of Polymer Science and Engineering and [⊥]Department of Chemical Engineering, National Taiwan University, Taipei 106, Taiwan

[§]Faculty of Engineering and Graduate School of Chemical Sciences and Engineering, Hokkaido University, Sapporo 060-8628, Japan

Supporting Information

ABSTRACT: Novel transparent conductive electrodes (TCEs) with copper (Cu)/silver (Ag) core/shell nanofibers (NFs) containing random, aligned, and crossed structures were prepared using a combination of electrospinning (ES) and chemical reduction. The ES process was used to prepare continuous copper nanofibers (Cu-NFs), which were used as core materials and were then immersed in silver ink (Ag ink) to form a protective layer of Ag to protect the Cu-NFs from oxidation. The Ag shell layer protected the Cu-NFs against oxidation and enhanced their conductivity. Such Cu/Ag core/shell webs can be easily transferred on the flexible matrix and can be applied in TCEs. The metal NF webs of different structures exhibited various degrees of conductivity and followed the order random type > crossed type > aligned type; however, the order with respect to transmittance (T) was inverse. The aligned nanowire networks exhibited a high T of over 80%, and the random ones exhibited a low sheet resistance of less than 10^2 Ω/sq (the best value is 7.85 Ω/sq). The present study demonstrated that TCEs based on Cu/Ag core/shell NF webs have considerable flexibility, transparency, and conductivity and can be applied in novel flexible light-emitting diode devices and solar cells in the future.

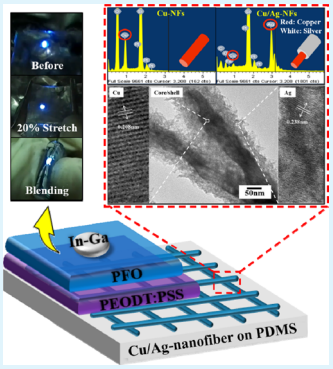

KEYWORDS: *transparent conductive electrodes, electrospun, nanofibers, electroless plating method, copper, silver*

INTRODUCTION

Transparent conductive electrode (TCE) films play critical roles in various electronic applications such as light-emitting diodes (LEDs), touch screen panels, and solar cells.[1,2] Sheet resistance (R_s) and optical transmittance (T) are two key parameters that determine the application of TCEs. Indium tin oxide (ITO) is a typical transparent conductive material because of its low R_s and favorable T; however, ITO exhibits several weaknesses such as brittleness, high refractive index, high processing temperature, and high cost. Therefore, finding a suitable replacement for ITO has been an ongoing task. Here, we divide TCEs into two types. Type I TCEs are based on the thin-film morphology that is evident in some transparent conductive oxides[3] such as ITO, aluminum zinc oxide, graphene,[4] and conducting polymer.[5] Type II TCEs are based on the networks of one-dimensional nanomaterials such as carbon nanotubes (CNTs),[6] graphene nanoribbons,[7] and metal nanowires,[8] all of which have been identified as novel materials for replacing ITO in TCEs.[9] Among these, silver nanowire (AgNW) has been reported to be the most promising candidate because of its high optical transparency and electrical conductivity.[10−13] However, the potential for mass production of AgNW is limited by the high price of silver (US$505/kg). Another option is copper, which is 80 times cheaper (US$6.36/kg) than silver and exhibits an electrical resistivity (16.8 nΩ·m) almost as low as silver (15.9 nΩ·m).[14] Furthermore, many studies have concluded that copper nanowire (CuNW) TCEs possess several remarkable physical properties such as excellent electrical conductivity, optical transparency, and mechanical flexibility.[15−17] Therefore, CuNW TCEs have attracted considerable research attention because they appear to be a promising alternative to ITO and AgNW TCEs. However, there is one critical problem with CuNWs: they are easily oxidized by moisture and oxygen in the environment, which has a major detrimental effect on their conductivity.

Many studies have focused on using double metals or materials to enhance the performance of conductive films.

Received: October 24, 2018
Accepted: February 14, 2019
Published: February 14, 2019

DOI: 10.1021/acsami.8b18366
ACS Appl. Mater. Interfaces 2019, 11, 10118−10127

Xiong et al. reported AgNW-iongel composite electrodes, which retards the oxidation process and elevates the air stability to a considerable extent.[18] Lee et al. utilized CNTs to overcome the transparency issue and also generated AgNW percolation networks by vacuum filtration process overlapped with CNT percolation networks to generate significant conductive electrodes.[19] Recently, Cu/Ag-based electrodes have been intensively studied by various methods because of its excellent electrical conductivity and easy availability and for improving the oxidation resistance for Cu electrodes. For example, Lee et al.[20] and Shang et al.[21] utilized a two-step process consisting of thermal decomposition and galvanic displacement methods to prepare Cu/Ag core/shell nanoparticles. Cu/Ag core/shell nanoparticles have better electrical property, higher thermal stability, and superior oxidation stability than the Cu nanoparticles because of the Ag shell coated cover Cu core. Although these Cu/Ag-based nanoparticle materials were substantial advancements, they were still difficult to be exploited in TCEs because of their poor transparency. Another work by Wei et al. revealed Cu/Ag core/shell NWs for flexible electronics with excellent oxidation resistance by using galvanic replacement reaction at room temperature without any heating, stirring, and dispersant.[22] On the other hand, Wiley et al. reported that the room-temperature and solution-phase process can be used to coat Cu NWs with shells of gold, silver, or platinum, which did not degrade the properties of Cu NWs.[23] Subsequently, Li et al. reported printable and flexible Cu/Ag alloy electrodes by using Cu/Ag hybrid ink and a low-temperature fabrication process of precuring, followed by rapid photonic sintering, which revealed high conductivity (3.4 $\mu\Omega$·cm) and ultrahigh oxidation resistance in an air atmosphere.[24] These previous studies have indicated that composite materials can considerably improve the performance, but in some cases, the process is extremely complicated or the instrumentation tends to be expensive. Most important of all, some literatures reported that Cu-Ag-based electrode containing core-shell nanoparticles, NWs, or hybrid ink exhibited good transparent and conductive performance, but very few ones talked about their practical application such as flexible optoelectronic devices.

The electrospinning (ES) technique can be used to prepare polymers into NF webs, providing an easy method to form a continuous NF web with many advantages such as low cost, flexibility, uniform diameter, long length, nanoscale diameter (10−1000 nm), and high specific surface area.[25−27] These advantages have motivated extensive studies concerning sensory applications that involve the sensing of pH levels,[28] temperatures,[29,30] nitric oxide gases,[31] and metal ions.[32−35] Using ES, various fluorescent sensor-based polymer NF webs for sensing pH and metallic ions, such as Hg^{2+}, Fe^{3+}, Zn^{2+}, and Cu^{2+}, were successfully prepared by our group.[32−35] Depending on the requirements of a particular application, the morphology can be fine-tuned with respect to the following characteristics: core shell, porosity, hollow, aligned, crossed, and random fiber structure. These multifunctional electrospun NF webs can be used in various fields such as environmental management, tissue engineering, and numerous optoelectronic devices.[36−41] Researchers have reported metal−polymer composite electrospun NF webs prepared from polymers blended with AgNWs and AgNPs, which have gained considerable attention in developing TCEs. Yi Cui group successfully utilized Cu-NF to fabricate high-performing TCEs through ES. Cu-NF webs have ultrahigh aspect ratios and a fused crossing point with ultralow junction resistances, which result in lower R_s at high T, for example, 50 Ω/sq at 90%.[42] Recently, An et al. successfully produced silver-decorated and palladium-coated Cu-electroplated polymer fibers via the combination of electrospinning, electroplating, and ion-exchange techniques.[43] This is the only study that has described the application of Cu-NF or Cu/metal-NF webs in TCEs by using the ES process. These studies propelled us to fabricate electrospun-based TCEs by employing the core/shell architecture using a combination of ES and chemical reduction.

To produce metal electrospun NF webs, Cu may be the best candidate because it is not only cheaper than Ag but also has a low R_s. However, Cu has a serious limitation: it is easily oxidized by O_2, resulting in a major decrease in its conductivity (Figure 1a). Herein, we proposed a novel strategy in which

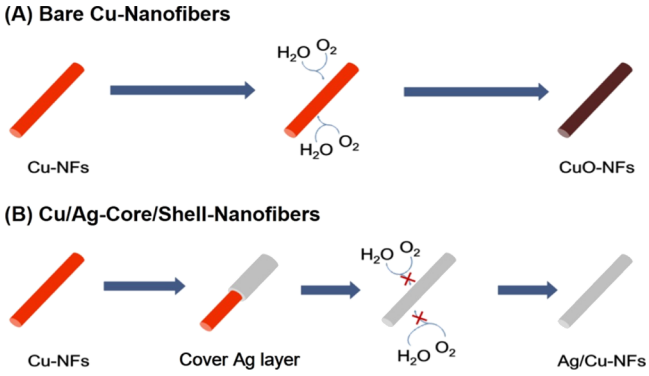

Figure 1. Schematics comparing the oxidation resistance of Cu/Ag core/shell NFs and bare Cu-NFs. (A) Bare Cu-NFs and (B) Cu/Ag-core/shell NFs.

TCEs were prepared from Cu/Ag core/shell NF webs by using a combination of ES and chemical reduction, which is an easy and cheap method for forming Ag layers to protect Cu-NFs from oxidation, as depicted in Figure 1b.

We introduced a novel TCE based on Cu/Ag core/shell metal NFs that were characterized by low cost, high conductivity, excellent transparency, and high stability through the combination of a reduction−oxidation heating process and ES. The electrical traits and transparency of the Cu/Ag core/shell metal NFs with different morphologies (random, crossed, and aligned type) were explored and compared. The electrospun NFs were prepared from $CuAc_2$/polyvinylpyrrolidone (PVP) that were thermally treated to oxidize them into CuO and then reduce into Cu. After the oxidation−reduction reaction, the Cu fibers were immersed into Ag ink, resulting in Cu/Ag core/shell metal NFs, as depicted in Figure 1. The as-prepared Cu/Ag core/shell metal NFs exhibited a high T of approximately 80% and lower R_s of 102 Ω/sq. The morphology of the prepared Cu/Ag core/shell metal NFs was characterized using field emission scanning electron microscopy (FE-SEM) and high-resolution transmission electron microscopy (HR-TEM). The Cu-NFs and Cu/Ag core/shell metal NFs were analyzed using X-ray diffraction (XRD) and energy dispersive X-ray spectroscopy (EDX) mapping to demonstrate that CuO NFs were successfully turned into Cu-NFs and Cu/Ag core/shell metal NFs. The transparency and R_s were analyzed on the basis of the ultraviolet−visible (UV−vis) light spectrum by using a Keithley 4200 semiconductor parametric analyzer. Experimen-

DOI: 10.1021/acsami.8b18366
ACS Appl. Mater. Interfaces 2019, 11, 10118−10127

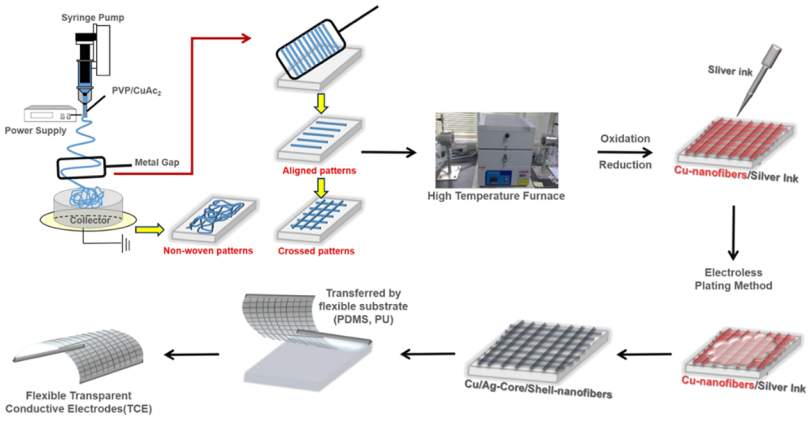

Figure 2. Experimental step of the process to form Cu/Ag core/shell NFs.

tal results indicated that compared with Cu-NFs, Cu/Ag core/shell NFs significantly enhanced the conductivity and chemical stability, maintained operational conductivity for a long time under an atmospheric environment, and could be applied to flexible TCEs for novel flexible LED devices and solar cells.

EXPERIMENTAL SECTION

Materials. Polyvinylpyrrolidone (PVP, M_w = 1,300,000, 99% hydrolyzed), Copper(II) acetate, methanol (HPLC, 99.9%), and ammonium hydroxide solution (ACS reagent, 28.0%−30.0% NH_3 basis), and Ag nitrate (99% hydrolyzed) were obtained from Sigma-Aldrich. Poly[9,9-dioctylfluorenyl-2,7-diyl] (PFO; American Dye Source, ADS129BE) was stored in a vacuum prior to use. Polydimethylsiloxane (PDMS; DOW-CORNING, SYGARD-184AB) was stored at 4 °C prior to use. The high-conductivity poly(3,4-ethylene dioxythiophene) polystyrene sulfonate (PEDOT:PSS) (Clevios, PH1000) and indium−gallium eutectic (99.99%) were purchased from Sigma-Aldrich.

Preparation of $CuAc_2$/PVP-NFs. PVP was first dissolved in DI water to create a polymer solution in which the concentration was 10 wt %; then, various concentrations—10, 15, and 20 wt %—were mixed with $CuAc_2$. Then, we used the simple ES process to produce electrospun NFs (Figure 2). A metallic needle was connected to a high-voltage power supply, and a piece of aluminum foil was placed 20 cm below the tip of the needle to collect NFs. The spinning voltage was set at 12.9 kV. The feed rate of the solution was 1 mL/h. After 40 min, random electrospun PVP NFs were collected on the aluminum foil that covered the Cu plate. Aligned and crossed PVP NFs were collected on a parallel Cu plate, which was covered with the aluminum foil. All experiments were performed at room temperature and at a relative humidity of approximately 20%.

Preparation of Cu-NFs by the Reduction−Oxidation Heating Process. Cu/Ag core/shell metal NFs were prepared as follows. $CuAc_2$/PVP-electrospun NFs were converted into Cu-NFs by using the reduction−oxidation heating process. The reduction−oxidation heating process was separated into two steps: (1) the oxidation step and (2) the reduction step. In the oxidation step, after ES, PVP/$CuAc_2$-NF membranes were placed in the quartz boat and heated at a rate of 2 °C/min, and the heat was increased from 30 to 250 °C; they were then held at the maximum heat for 1 h in a constant flow of gas composed of 80% nitrogen and 20% oxygen. After that, PVP/$CuAc_2$-NFs were heated to 500 °C at a rate of 5 °C/min for 2 h in air. Copper acetate ($CuAc_2$) was converted into copper oxide (CuO), and the PVP polymer was pyrolyzed into carbon dioxide. In the reduction step, CuO-NF membranes were placed in the quartz boat and heated at a rate of 5 °C/min, and the heat was increased from 30 to 300 °C in a constant flow of argon/hydrogen gas; they were then maintained at 300 °C for 1 h in the tube furnace. After hydrogen reduction, Cu-NF membranes were fabricated on the glass substrate.

Preparation of Cu/Ag Core/Shell Metal NFs from Ag Electroless Deposition (Cu-NFs Change to Cu/Ag Core/Shell NFs). Cu/Ag core/shell NFs were prepared using the electroless plating method. To prepare an Ag precursor, an $Ag(NH_3)_2^+$ solution was used. First, stoichiometrically excess $AgNO_3$ (+99%, Sigma-Aldrich, St. Louis, MO) was weighed and dissolved in DI water to yield 30 g/L of $AgNO_3$ solution. Subsequently, NH_4OH (14.8 M, EMD Millipore Chemicals) was added into $AgNO_3$ solution drop by drop with vigorous stirring until the yellow precipitate disappeared and the solution became clear. Cu-NFs were then immersed into the $Ag(NH_3)_2^+$ solution. Second, the Ag amine reagent was added drop by drop onto the Cu-NF mat, which was then immersed in DI water to wash the Ag amine reagent. After immersion, Cu/Ag core/shell-NFs were extracted from DI water and dried using an air gun.

$$AgNO_3 + 2NH_4OH \rightarrow [Ag(NH_3)_2]NO_3 + H_2O \quad (1)$$

$$Cu + 2[Ag(NH_3)_2]NO_3 \rightarrow [Cu(NH_3)_4](NO_3)_2 + 2Ag\downarrow \quad (2)$$

Process of Preparing Polymer Light-Emitting Devices. PDMS films were prepared by coating the precursors (10:1) onto glass and curing at 100 °C for 5 min. PDMS substrates were oxygen-plasma treated for 3 min. Aqueous PEDOT:PSS was mixed with dimethyl sulfoxide solution at the desired weight ratio and stirred at 1500 rpm for 30 min. The PEDOT:PSS solution was spin-coated on PDMS at 1500 rpm for 30 s and annealed at 80 °C for 10 min to yield 45−50 nm thin films. PFO was dissolved in chlorobenzene (10 mg/mL). An emissive PFO polymer layer was spin-coated further at 1000 rpm for 1 min. The films were then annealed at 80 °C for 10 min. Device fabrication and testing were conducted in an atmospheric environment (the direction of current flow was from In−Ga to PDMS). Current density−voltage and luminance−voltage characteristics were measured using a Keithley 2400 source meter and a silicon photodiode. The silicon photodiode was further calibrated using a photo research PR-670 spectroradiometer.

Characterization. The structure of the Cu/Ag core/shell NF was observed using a Hitachi H-7100 (operating at 100 kV) transmission electron microscope; the morphology of the prepared electrospun fibers was characterized using FE-SEM (Hitachi S-4800; cold-field emission scanning electron microscope), and images were taken using a microscope operated at an accelerating voltage of 10 kV. The samples were sputtered with Pt and then analyzed using a QUANTAX ANNULAR XFlash QUAD FQ5060 system, and optical transmittance spectra for Cu and Cu/Ag core/shell NFs were recorded using a UV−vis spectrophotometer (Hitachi U-4100). X-ray photoelectron spectra were collected on an ESCALab MkII X-ray photoelectron spectrometer using non-monochromatized Mg $K\alpha$ X-ray as the excitation source. The Cu-NFs and the Cu/Ag core/shell NFs after electroless plating were investigated through transmission-mode XRD at beamlines 17 A and 01 C of National Synchrotron Radiation Research Center, Taiwan. R_s of Cu-NFs and Cu/Ag core/shell NFs were measured using a Keithley 4200 semiconductor

DOI: 10.1021/acsami.8b18366
ACS Appl. Mater. Interfaces 2019, 11, 10118−10127

parametric analyzer. These electrical measurements were performed in a nitrogen-filled glove box. The luminance of polymer LED (PLED) was measured in the ambient atmosphere by using a PR670 spectrophotometer with a Keithley 2400 Source Measure Unit connected to a dc-to-ac inverter purchased from Shanghai KPT Company.

RESULTS AND DISCUSSION

ES is a promising and straightforward technique for producing continuous fibers with diameters ranging from nanometers to a few micrometers; various architectures of Cu/Ag core/shell metal NFs can be readily prepared using this technique. We prepared Cu-NFs through ES. To ensure the quality of NFs, we tested three concentrations of $CuAc_2$/PVP-electrospun NFs. We found a beadlike shape of NFs when the concentration was 10 wt % because the polymer viscosity was too low to spin into NFs. Finally, we chose the concentration of 20 wt % to perform the experiment because this concentration yielded the best quality fibers, as shown in Figure S1, Supporting Information. The major problem for Cu-NFs is their oxidation after exposure to air. After being exposed to air, the sheet resistance (R_s) of Cu-NFs noticeably increased. Unlike aluminum oxide or nickel oxide, CuO grows as an island and then coalesces into a film, which then tends to have pinholes and microcracks. Therefore, the oxidation of Cu-NFs caused a substantial decrease in conductivity. Compared with the bulk or a film of Cu, the large surface area of Cu-NFs resulted in a more rapid rate of oxidation. To prevent the oxidation of Cu, we used the electroless plating method to coat an Ag layer on the Cu-NFs, which successfully solved this problem at a low cost compared with chemical vapor deposition (CVD)[44] or electroplating,[45] both of which are highly energy consumptive and expensive (Figure 1). Cu/Ag core/shell NFs fabricated by combining the ES technique and the electroless plating method exhibited high conductivity and maintained excellent transparency and can be applied to transparent electrodes and optoelectronics.

Figure 2 is a photograph depicting all experimental steps used to prepare Cu/Ag core/shell NFs. Precursor NFs with Cu acetate were dissolved in PVP; then, three types of composite $CuAc_2$/PVP-electrospun NFs (random, aligned, and crossed) were prepared using the ES technique. An aluminum foil was placed 20 cm below the tip of the needle to collect NFs. Then, $CuAc_2$PVP/-NF membranes were treated using the reduction−oxidation heating process to obtain Cu-NFs. Finally, Cu-NFs were dipped into an Ag ink solution to cover Cu-NFs with Ag. After immersion, Cu-NF membranes converted into Cu/Ag core/shell NFs and were dried using an air gun.

Scanning electron microscopy (SEM) and energy dispersive spectroscopy (EDS) mapping analysis were used to capture the images of $CuAc_2$/PVP NFs, Cu-electrospun NFs, and Cu/Ag core/shell NFs, as displayed in Figure 3. The best morphology of the $CuAc_2$/PVP NF concentration was exhibited at 200 mg/mL. Here, we prepared 200 mg/mL of $CuAc_2$/PVP-NFs through ES (Figure 3a) and then put them into the furnace. The $CuAc_2$/PVP-NFs were heated in air at 500 °C for 1 h at a heating rate of 2 °C/min; then, the precursor of Cu was turned into CuO. After cooling to room temperature, the furnace was purged by the mixture gas of hydrogen: argon (9:1) and annealed at 300 °C for half an hour at a heating rate at 2 °C/min. After reduction, CuO-NFs were converted into Cu-NFs as displayed in Figure 3b. Cu-NFs were somewhat damaged after heat treatment in the furnace at 500 °C. The damaged

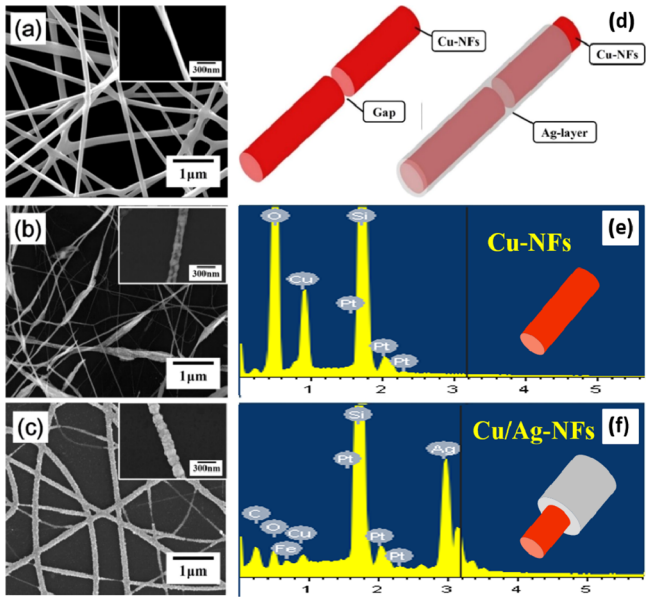

Figure 3. SEM image of (a) $CuAc_2$/PVP-NFs, (b) Cu-NFs, and (c) Cu/Ag core/shell NFs, and the high magnification of SEM images at the right. (d) Schematic of Ag recovery mechanism; the EDX spectrum of (e) Cu-NFs and (f) Cu/Ag core/shell NFs.

NFs increased the R_s of Cu-NFs. The next step was to immerse Cu-NFs into the Ag-reactive solution to form the Ag protective layer to prevent Cu oxidation. The SEM image of Cu/Ag core/shell NFs is displayed in Figure 3c. The composite Cu/Ag core/shell NFs became continuous again (schematic illustration in Figure 3d). The EDX spectra in Figure 3e,f reveal the peaks of Cu and Ag that indicated that they successfully covered PVP-NFs depicted in Figure 3b,c. As depicted in Figure 4, $CuAc_2$/PVP-electrospun NFs were fabricated at an

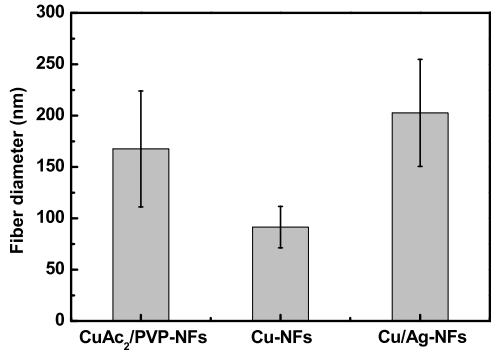

Figure 4. Average fiber diameter of $CuAc_2$/PVP-NFs, Cu-NFs, and Cu/Ag-NFs.

average diameter of 167 ± 56.46 nm. After annealing with hydrogen gas, Cu-NFs were fabricated. Their average diameters were 91 ± 20.16 nm. Because of thermal treatment, the polymer was evaporated into CO_2 and the diameter decreased considerably. After performing the electroless plating method, the Ag protective layer covered the Cu-NFs, and the diameter of Cu/Ag core/shell NFs was increased to 202 ± 52.05 nm. Note that the fiber diameter of Cu/Ag-NFs can be optimized by tuning the time factors for encapsulating the Ag shell on Cu-NFs. If we use lesser time than the optimized time for electroless plating, the shell formation is not

DOI: 10.1021/acsami.8b18366
ACS Appl. Mater. Interfaces 2019, 11, 10118−10127

uniform, and this might retard the oxidation resistance of the core/shell structure and lower the conductivity.

Figure 5 a,b presents the high-resolution SEM images of the Cu/Ag core/shell nanostructure. Cu-NF lattices were observed

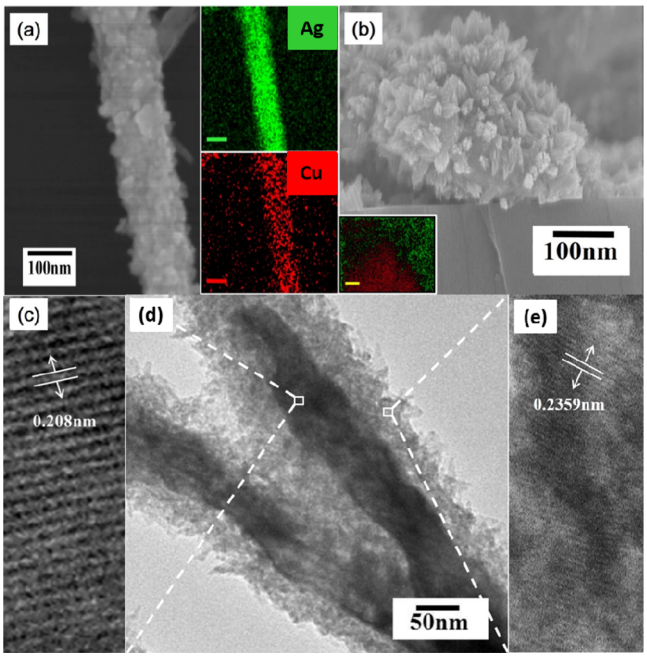

Figure 5. (a) High-resolution SEM image inverse fast Fourier transform (FFT) image of the middle of the Cu/Ag core/shell nanostructure. (b) High-resolution TEM image inverse FFT image of the edge of Cu/Ag core/shell nanostructure. (c) TEM image of the Cu/Ag core/shell nanostructure. (d) HR-TEM image inverse FFT image of the edge of the Cu/Ag core/shell nanostructure. (e) TEM image of the Cu/Ag core/shell nanostructure.

internal to the core/shell nanostructure of Cu/Ag-NFs. Their inset figure shows the corresponding EDS mapping (green: Ag; red: Cu). As shown in Figure 5b, the sectional fiber morphology indicates the Ag cover in the outer layer of the fiber and Cu located in the core layer. Besides, as evidenced in Figure 5c,d, the HR-TEM images of the Cu/Ag-NFs show that the lattice distance was 0.208 nm corresponding to the lattice distance value of the (111) plane of Cu-NFs (Figure 5c). At the edge of the Cu/Ag core/shell nanostructure depicted in Figure 5d, Ag layers were observed. The lattice constant of Ag protective layers in the shell was estimated to be 0.2359 nm, as presented in Figure 5e. Figure 6a,b illustrates the XRD patterns of Cu-NFs and Cu/Ag core/shell NFs. As evidenced in Figure 6a, the fabricated CuO NFs were successfully converted into Cu-NFs. This proved that the hydrogen reduction process was successful for converting CuO into Cu. With the electroless plating treatment, Cu-NFs were converted into Cu/Ag core/shell NFs and exhibited distinct diffraction peaks of Ag in the XRD pattern shown in Figure 6b. Because Ag was completely covered onto Cu-NFs, the XRD pattern was dominated by the diffraction of Ag, which resulted from the stronger signal peak intensity of the Ag cover on Cu. These TEM and XRD results clearly confirmed that the Cu/Ag core/shell nanostructure can be successfully synthesized using the electroless plating process, which is easier for producing the protective layer than the low-temperature plasma-enhanced CVD process[44] or the atomic layer deposition process.[46]

Cu/Ag core/shell NF TCEs were stable because of Ag shell protection. As shown in Figure 7, we first kept Cu-NFs and Cu/Ag core/shell NFs at a room temperature of approximately 28 °C and an average humidity of approximately 60%. R_s values were measured using a four-terminal configuration to eliminate the contact resistances. Each stripe-shaped contact was made by a conductive Ag paint, which develops a typical Ohmic contact resistance of lesser than 1 Ω. As depicted in Figure 7a, the R_s of Cu-NFs increased by approximately 1.7-fold compared with the initial resistance R_0, whereas the R_s of Cu/Ag core/shell NFs only slightly increased. To accelerate the rate of oxidation, the resistances were further measured in a harsher environment where the relative humidity and the temperature were controlled at 80 ± 10% and 85 °C, whose values are even higher than those reported in the literature,[47−49] as shown in Figure 7b.

We then discuss the morphologies and properties of the NFs fabricated in random, aligned, and crossed structures using the uniaxial ES technique. SEM and EDS mapping were used to capture the images of the processed NFs, as displayed in Figure 8. The $CuAc_2$ precursor blending in the as-spun NFs with the thermal treatment led to oxidation into CuO and then reduction into Cu. The smallest diameter of NF led to the highest orientation of the $CuAc_2$ precursor because of the geometrical confinement. According to Figure 8a, we tuned the best concentration of the $CuAc_2$/PVP-NFs, and then we changed the collecting plate from disc to parallel to collect the aligned $CuAc_2$/PVP-NFs, as shown in Figure 8b. Hence, we collected the NFs on the aluminum disc, which had a rectangle gap with the area 3 cm × 1.5 cm. The NFs, which had crossed over the rectangle gap, were lined up on the aluminum disc

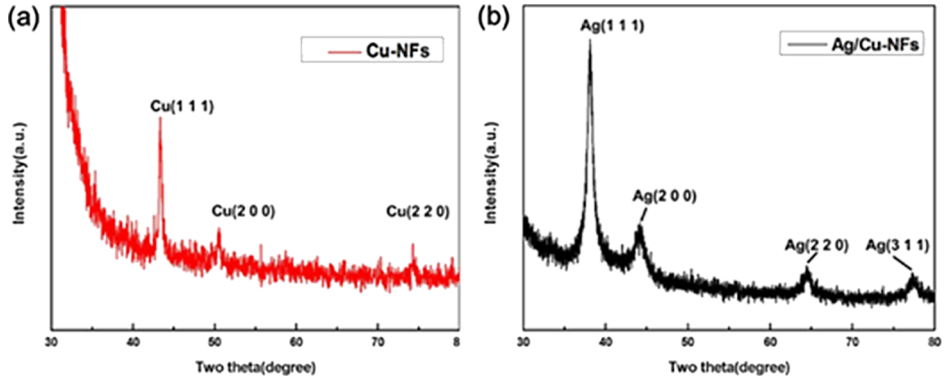

Figure 6. XRD patterns of (a) CuO-NFs, (b) Cu-NFs, and (c) Cu/Ag core/shell NFs.

DOI: 10.1021/acsami.8b18366
ACS Appl. Mater. Interfaces 2019, 11, 10118−10127

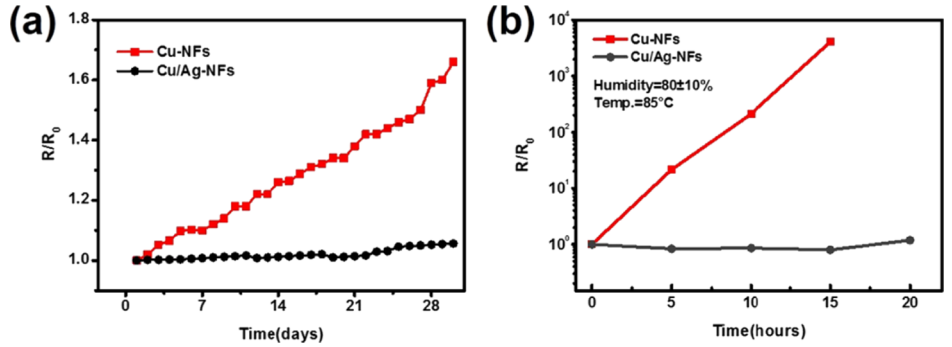

Figure 7. Oxidation test of Cu-NFs and Cu/Ag core/shell NFs at (a) room temperature and (b) humidity 80 ± 10% and 85 °C.

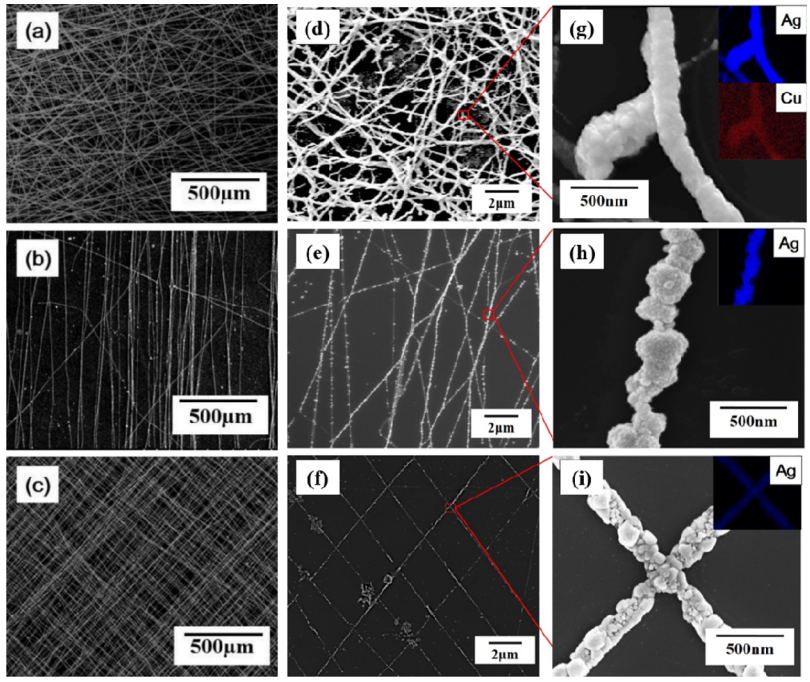

Figure 8. $CuAc_2$/PVP-electrospun NFs with different morphologies: (a) random (b) aligned and (c) crossed. Cu/Ag core/shell NFs with different morphologies: (d) random (e) aligned and (f) crossed. Magnified SEM images with different morphologiesy and the EDX analysis: (g) random, (h) aligned, and (i) crossed.

and then were covered on the hard substrate. Finally, we repeated the step with 90° rotation to collect the crossed morphology, as shown in Figure 8c.

The patterns of the Cu/Ag core/shell NFs after annealing and coating of the Ag protective layer, as exhibited in Figure 8d–f, are similar to those of $CuAc_2$/PVP-NFs but with higher roughness on the surface because of the removal of PVP after thermal treatment. The $CuAc_2$ had oxidized into CuO nanoparticles, but not the same that we use in the ES process to confine the copper oxide nanoparticles packed in the path of elcrospun NF and not scattered everywhere, as depicted in Figure 8g–i. The top right of Figure 8g–i of the SEM images presents the EDX mapping of various morphologies to confirm the element of NFs. As illustrated in the EDX mapping presented in Figure 8g–i, a blue dot appeared in the EDX mapping, which proved that Ag signals on NFs (Figure 8g) were a little different in the EDX mapping.

The transmittances of the Cu-NFs and Cu/Ag core/shell NFs in different web structures are depicted in Figure 9. The transmittance was dependent on the empty areas between NFs. When the light passed through the films, the nodes of NFs block the light and cause the transparency to decrease; and therefore, the more the nodes in NF films, the less the transmittance. Figure 9a shows that the transparency is in the order of aligned NFs > crossed NFs > random NFs, following the number of nodes in the films. After electroless plating, the Ag protective layer on Cu-NFs increased the diameter of the fibers, and the transparency decreased by approximately 10%. The transmittance was plotted against R_s in Figure 9b. After Ag electroless plating, the R_s decreased because of the implementation of the Ag protective/conductive layer that connected the discontinuous Cu-NFs. However, the transparency of all Cu/Ag core/shell NFs is above 75%, similar to the high transparency of ITO. As presented in Figure 9b, a random network of Cu-NFs and Cu/Ag core/shell NFs outperformed all other TCEs in terms of R_s but had a lower transmittance because of the larger number of intersection points, compared with aligned- or crossed-type ones. The intersection points can provide multiple pathways for charge transport. So, the conductivity is in order of random NFs > crossed NFs > aligned NFs, which is in contrast to the results of their transparency. As shown in the schematic illustration in

DOI: 10.1021/acsami.8b18366
ACS Appl. Mater. Interfaces 2019, 11, 10118–10127

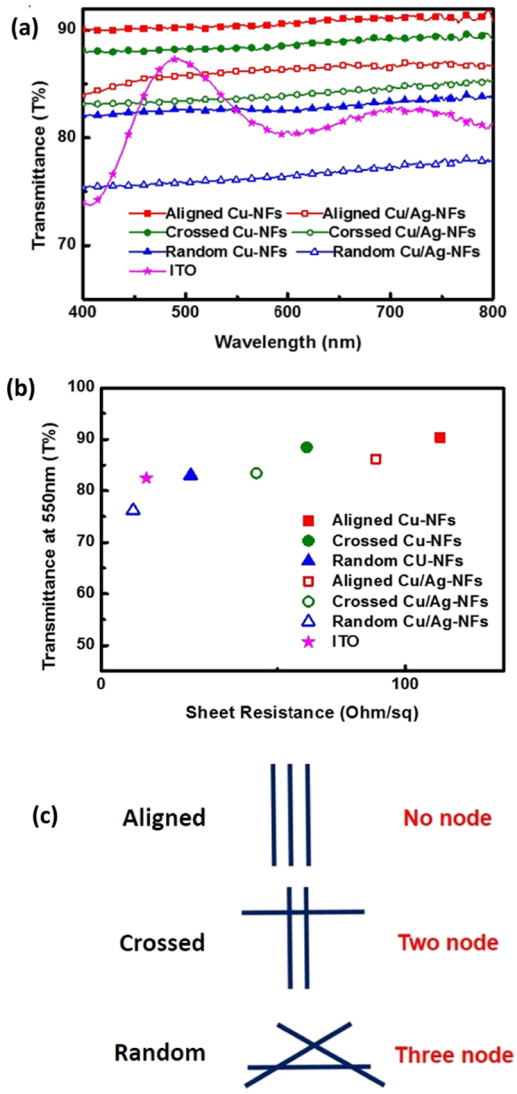

Figure 9. (a) Transparency test of Cu-NFs and Cu/Ag core/shell NFs with three different morphologies (aligned, crossed, and random). (b) Transmittance is plotted against sheet resistance with different morphologies (random, aligned, and crossed) of Cu-NFs and Cu/Ag core/shell NFs. (c) Node theory of transmittance.

Figure 9c, the number of intersection points is zero for three aligned NFs, two points for three cross NFs, and three points for three random NFs, representing the node theory of transmittance. After covering with the Ag protective layer, the diameter, path cross-section, and conductivity increased, but the empty gap area of the NF films decreased. Although more area blocked the light from passing through the film, transmittance remained above 75%, which was sufficient for TCEs, and the sheet resistance (R_s) of all Cu/Ag core/shell NFs is below 100 Ω/sq.

There are two key parameters for TCEs. One is low R_s and the other is high transmittance. The fiber collection time in the ES process can be used to tune the R_s and transmittance. In general, as the collection time increases, R_s increases while the transmittance decreases. We prepared the films with five different collection times: 15, 30, 45, 60, and 75 min. The transparencies of the NFs are compared in Figure 10. Comparing the various time points, the best we can get is at 45 min, which has lower R_s and transparency is still kept

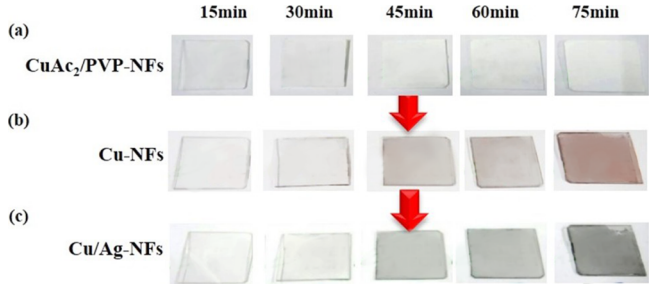

Figure 10. Digital photos to show the color change of the samples: (a) $CuAc_2$/PVP-NFs (the precursor samples), (b) Cu-NFs fabricated by thermal treatment in the hydrogen (H2) atmosphere at 300 °C (red color), and (c) Cu/Ag core/shell NFs, fabricated by the electroless plating process with immersed silver ink for 15 s.

around 80%. As shown in Figure 10c, we can easily observe transparency on the digital photos of Cu/Ag core/shell NFs prepared from the collecting ES time below 45 min. It means the light scattering does not affect their transparency.

As depicted in Figure 11, we controlled the fiber density to tune the optimum R_s and the transparency of Cu-NFs and Cu/

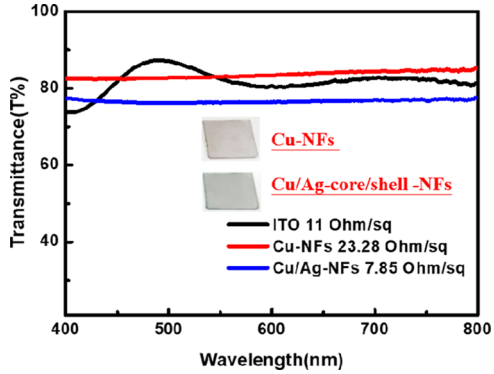

Figure 11. Best tuning of Cu-NFs and Cu/Ag core/shell NFs.

Ag-NFs. In this experiment, electrospun NFs were collected after approximately 45 min. After thermal treatment, oxidation, and reduction, R_s of Cu/Ag core/shell NFs was approximately 7.85 Ω/sq and transparency at 550 nm was approximately 82%, which is suitable to produce optoelectronic devices. It is worth noting that Cu/Ag core/shell NFs exhibit an R_s of 7.85 Ω/sq, which is almost three times lower than that of bare Cu-NFs (23.28 Ω/sq), and is attributed to the conformal Ag encapsulation on Cu-NFs. Our work presents a low R_s value of 7.85 Ω/sq compared with other AgNW-based reported in the literature.[50−52]

In order to produce the flexible optoelectronic device, Cu/Ag: core/shell NFs was transferred to other flexible materials (e.g., Polyurethane (PU) or Polydimethylsiloxane (PDMS)), and chemical stability of the Cu/Ag: core/shell structure was studied with identical optimized device process under ambient atmosphere, showing in Figure 12. Because of their large aspect ratios, nanoscale diameters, and the metallic bonding nature of Cu/Ag-NFs, such TCEs should demonstrate excellent flexibility, stability, and stretching. Transparent Cu/Ag-NF electrodes on PDMS substrates can be successfully fabricated by simply transferring Cu/Ag-NF networks to PDMS. In our work, we used Cu/Ag-NFs on PDMS for the anode and PEDOT:PSS for the hole-transport layer. PFO (M_w = 40 000−150 000) was chosen to be the emission material, and eutectic

DOI: 10.1021/acsami.8b18366
ACS Appl. Mater. Interfaces 2019, 11, 10118−10127

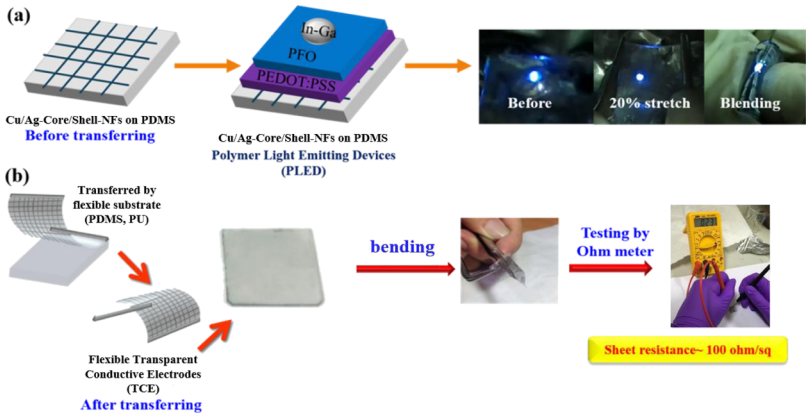

Figure 12. Application of Cu/Ag core/shell NF electrodes in semitransparent and flexible PLEDs; (a) application of device and structure and (b) transferred by PDMS.

indium−gallium was chosen to be the cathode. As shown in Figure 12a, these novel NF TCEs were not only stable but also flexible. The resistance value of Cu/Ag-NF electrodes remained almost the same even after transferring to PDMS and bending around 100 times, as shown in Figure 12b. The as-prepared devices emitted visible blue light starting at 6 V. The luminance intensity increased with voltage and obtained a maximum value of 62.53 cd/m^2 at 10 V. The current efficiency also exhibited a rising trend with applied voltage and saturated at 0.045 cd/A after about 12 V, as shown in Figure S2 (Supporting Information). We demonstrated that intrinsically stretchable PLEDs had a high degree of transparency and flexible bending. Cu/Ag-NF electrodes were mechanically robust and could be stretched up to 20% strain without any cracks, resulting in PLEDs still emitting after stretching. Thus, in this study, the novel Cu/Ag core/shell NF electrodes could easily be transferred to any other substrate for a versatile shape design. The excellent flexibility performance of transparent conductive Cu/Ag-NFs may open new avenues for future foldable electronics.

CONCLUSIONS

In summary, we successfully fabricated various structures (random, aligned, and crossed types) of Cu/Ag core/shell NFs by using the Ag electroless plating process to coat the Ag protective layer onto the electrospun Cu-NF. The Ag protective layer considerably enhanced the stability of the fibers against oxidation and improved its conductivity. R_s of Cu-NFs was 23.28 Ω/sq, and the R_s of Cu/Ag core/shell NFs was 7.85 Ω/sq. R_s decreased by a factor of 3, indicating that the conductivity was largely enhanced. The Ag protective and conductive layers substantially prevented Cu-NFs from undergoing thermal oxidation at a temperature of 85 °C and a humidity of 80 ± 10%. Given the extraordinary performance and the cost effectiveness of electrospun Cu-NFs as transparent electrodes, this protective method provided a critical advantage for Cu-NFs to replace ITO in the industry and in commercial uses. In addition, our study demonstrated that applying an Ag protective layer on the surfaces of Cu-NFs was also a general and effective route to improve the chemical stability and conductivity of other nanoscaled metals. By combining the ES processing technology and the electroless plating method, we demonstrated the high conductivity and excellent transparency of the fibrous films that can be applied to transparent electrodes and flexible optoelectronics in the future.

ASSOCIATED CONTENT

Supporting Information

The Supporting Information is available free of charge on the ACS Publications website at DOI: 10.1021/acsami.8b18366.

FE-SEM images of $CuAc_2$/PVP electrospun NFs with various concentrations of 10, 15, and 20 wt % and PLEDs optoelectronic analysis comprising current density−voltage, luminance−voltage, and current efficiency−voltage characteristics(PDF)

AUTHOR INFORMATION

Corresponding Authors

*E-mail: kuocc@mail.ntut.edu.tw. Phone: 886-2-27712171 ext. 2407. Fax: 886-2-27317174 (C.-C.K.).
*E-mail: satoh@eng.hokudai.ac.jp (T.S.).
*E-mail: shtung@ntu.edu.tw (S.-H.T.).

ORCID

Chi-Ching Kuo: 0000-0002-1994-4664
Ying-Chih Liao: 0000-0001-9496-4190
Toshifumi Satoh: 0000-0001-5449-9642
Shih-Huang Tung: 0000-0002-6787-4955

Author Contributions

#D.-H.J. and P.-C.T. contributed equally to this work.

Notes

The authors declare no competing financial interest.

REFERENCES

(1) Lee, H.; Lee, D.; Ahn, Y.; Lee, E.-W.; Park, L. S.; Lee, Y. Highly Efficient and Low Voltage Silver Nanowire-Based OLEDs Employing a N-Type Hole Injection Layer. *Nanoscale* **2014**, *6*, 8565−8570.
(2) Wu, H.; Kong, D.; Ruan, Z.; Hsu, P.-C.; Wang, S.; Yu, Z.; Carney, T. J.; Hu, L.; Fan, S.; Cui, Y. A Transparent Electrode Based on a Metal Nanotrough Network. *Nat. Nanotechnol.* **2013**, *8*, 421−425.
(3) Ellmer, K. Past Achievements and Future Challenges in the Development of Optically Transparent Electrodes. *Nat. Photonics* **2012**, *6*, 809−817.
(4) Kim, K. S.; Zhao, Y.; Jang, H.; Lee, S. Y.; Kim, J. M.; Kim, K. S.; Ahn, J.-H.; Kim, P.; Choi, J.-Y.; Hong, B. H. Large-Scale Pattern Growth of Graphene Films for Stretchable Transparent Electrodes. *nature* **2009**, *457*, 706−710.

DOI: 10.1021/acsami.8b18366
ACS Appl. Mater. Interfaces 2019, 11, 10118−10127

(5) Ma, C.; Song, Y.; Shi, J.; Zhang, D.; Zhai, X.; Zhong, M.; Guo, Q.; Liu, L. Preparation and One-step Activation of Microporous Carbon Nanofibers for Use as Supercapacitor Electrodes. *Carbon* **2013**, *51*, 290−300.
(6) He, H.; Li, X.; Wang, J.; Qiu, T.; Fang, Y.; Song, Q.; Luo, B.; Zhang, X.; Zhi, L. Reduced Graphene Oxide Nanoribbon Networks: a Novel Approach Towards Scalable Fabrication of Transparent Conductive Films. *Small* **2013**, *9*, 820−824.
(7) Liu, C.-H.; Yu, X. Silver Nanowire-Based Transparent, Flexible, and Conductive Thin Film. *Nanoscale Res. Lett.* **2011**, *6*, 75.
(8) Hsu, P.-C.; Kong, D.; Wang, S.; Wang, H.; Welch, A. J.; Wu, H.; Cui, Y. Electrolessly Deposited Electrospun Metal Nanowire Transparent Electrodes. *J. Am. Chem. Soc.* **2014**, *136*, 10593−10596.
(9) Stewart, I. E.; Rathmell, A. R.; Yan, L.; Ye, S.; Flowers, P. F.; You, W.; Wiley, B. J. Solution-processed copper-nickel nanowire anodes for organic solar cells. *Nanoscale* **2014**, *6*, 5980−5988.
(10) De, S.; Higgins, T. M.; Lyons, P. E.; Doherty, E. M.; Nirmalraj, P. N.; Blau, W. J.; Boland, J. J.; Coleman, J. N. Silver Nanowire Networks as Flexible, Transparent, Conducting Films: Extremely High DC to Optical Conductivity Ratios. *ACS Nano* **2009**, *3*, 1767−1774.
(11) Hu, L.; Kim, H. S.; Lee, J.-Y.; Peumans, P.; Cui, Y. Scalable Coating and Properties of Transparent, Flexible, Silver Nanowire Electrodes. *ACS Nano* **2010**, *4*, 2955−2963.
(12) Lee, J.-Y.; Connor, S. T.; Cui, Y.; Peumans, P. Solution-Processed Metal Nanowire Mesh Transparent Electrodes. *Nano Lett.* **2008**, *8*, 689−692.
(13) Madaria, A. R.; Kumar, A.; Ishikawa, F. N.; Zhou, C. Uniform, Highly Conductive, and Patterned Transparent Films of a Percolating Silver Nanowire Network on Rigid and Flexible Substrates Using a Dry Transfer Technique. *Nano Res.* **2010**, *3*, 564−573.
(14) Rathmell, A. R.; Wiley, B. J. The Synthesis and Coating of Long, Thin Copper Nanowires to Make Flexible, Transparent Conducting Films on Plastic Substrates. *Adv. Mater.* **2011**, *23*, 4798−4803.
(15) Sachse, C.; Weiß, N.; Gaponik, N.; Müller-Meskamp, L.; Eychmüller, A.; Leo, K. ITO-Free, Small-Molecule Organic Solar Cells on Spray-Coated Copper-Nanowire-Based Transparent Electrodes. *Adv. Energy Mater.* **2014**, *4*, 1300737.
(16) Ye, S.; Rathmell, A. R.; Stewart, I. E.; Ha, Y.-C.; Wilson, A. R.; Chen, Z.; Wiley, B. J. A Rapid Synthesis of High Aspect Ratio Copper Nanowires for High-Performance Transparent Conducting Films. *Chem. Commun.* **2014**, *50*, 2562−2564.
(17) Zhang, D.; Wang, R.; Wen, M.; Weng, D.; Cui, X.; Sun, J.; Li, H.; Lu, Y. Synthesis of Ultralong Copper Nanowires for High-Performance Transparent Electrodes. *J. Am. Chem. Soc.* **2012**, *134*, 14283−14286.
(18) Xiong, W.; Liu, H.; Chen, Y.; Zheng, M.; Zhao, Y.; Kong, X.; Wang, Y.; Zhang, X.; Kong, X.; Wang, P.; Jiang, L. Highly Conductive, Air-Stable Silver Nanowire@Iongel Composite Films toward Flexible Transparent Electrodes. *Adv. Mater.* **2016**, *28*, 7167−7172.
(19) Lee, P.; Ham, J.; Lee, J.; Hong, S.; Han, S.; Suh, Y. D.; Lee, S. E.; Yeo, J.; Lee, S. S.; Lee, D.; Ko, S. H. Highly Stretchable or Transparent Conductor Fabrication by a Hierarchical Multiscale Hybrid Nanocomposite. *Adv. Funct. Mater.* **2014**, *24*, 5671−5678.
(20) Lee, C.; Kim, N. R.; Koo, J.; Lee, Y. J.; Lee, H. M. Cu-Ag core-shell nanoparticles with enhanced oxidation stability for printed electronics. *Nanotechnology* **2015**, *26*, 455601.
(21) Shang, S.; Kunwar, A.; Wang, Y.; Qi, X.; Ma, H.; Wang, Y. Synthesis of Cu@ Ag Core−Shell Nanoparticles for Characterization of Thermal Stability and Electric Resistivity. *Appl. Phys. A: Mater. Sci. Process.* **2018**, *124*, 492.
(22) Wei, Y.; Chen, S.; Lin, Y.; Yang, Z.; Liu, L. Cu-Ag core-shell nanowires for electronic skin with a petal molded microstructure. *J. Mater. Chem. C* **2015**, *3*, 9594−9602.
(23) Stewart, I. E.; Ye, S.; Chen, Z.; Flowers, P. F.; Wiley, B. J. Synthesis of Cu-Ag, Cu-Au, and Cu-Pt Core-Shell Nanowires and Their Use in Transparent Conducting Films. *Chem. Mater.* **2015**, *27*, 7788−7794.
(24) Li, W.; Hu, D.; Li, L.; Li, C.-F.; Jiu, J.; Chen, C.; Ishina, T.; Sugahara, T.; Suganuma, K. Printable and Flexible Copper-Silver Alloy Electrodes with High Conductivity and Ultrahigh Oxidation Resistance. *ACS Appl. Mater. Interfaces* **2017**, *9*, 24711−24721.
(25) Chen, Y.-Y.; Kuo, C.-C.; Chen, B.-Y.; Chiu, P.-C.; Tsai, P.-C. Multifunctional polyacrylonitrile-ZnO/Ag electrospun nanofiber membranes with various ZnO morphologies for photocatalytic, UV-shielding, and antibacterial applications. *J. Polym. Sci., Part B: Polym. Phys.* **2015**, *53*, 262−269.
(26) Kuo, C.-C.; Tung, Y.-C.; Lin, C.-H.; Chen, W.-C. Novel Luminescent Electrospun Fibers Prepared From Conjugated Rod-Coil Block Copolymer of Poly[2,7-(9,9-dihexylfluorene)]-block-Poly(methyl methacrylate). *Macromol. Rapid Commun.* **2008**, *29*, 1711−1715.
(27) Kuo, C.-C.; Lin, C.-H.; Chen, W.-C. Morphology and Photophysical Properties of Light-Emitting Electrospun Nanofibers Prepared from Poly(fluorene) Derivative/PMMA Blends. *Macromolecules* **2007**, *40*, 6959−6966.
(28) Kuo, C.-C.; Tung, Y.-C.; Chen, W.-C. Morphology and pH Sensing Characteristics of New Luminescent Electrospun Fibers Prepared from Poly(phenylquinoline)-block-Polystyrene/Polystyrene Blends. *Macromol. Rapid Commun.* **2010**, *31*, 65−70.
(29) Chiu, Y.-C.; Chen, Y.; Kuo, C.-C.; Tung, S.-H.; Kakuchi, T.; Chen, W.-C. Synthesis, Morphology, and Sensory Applications of Multifunctional Rod-Coil-Coil Triblock Copolymers and Their Electrospun Nanofibers. *ACS Appl. Mater. Interfaces* **2012**, *4*, 3387−3395.
(30) Chiu, Y.-C.; Kuo, C.-C.; Hsu, J.-C.; Chen, W.-C. Thermoresponsive Luminescent Electrospun Fibers Prepared From Poly-(DMAEMA-co-SA-co-StFl) Multifunctional Random Copolymers. *ACS Appl. Mater. Interfaces* **2010**, *2*, 3340−3347.
(31) Chen, L.-N.; Chiu, Y.-C.; Hung, J.-J.; Kuo, C.-C.; Chen, W.-C. Multifunctional Electrospun Nanofibers Prepared from Poly((N-isopropylacrylamide)-co-(N-hydroxymethylacrylamide)) and Their Blends with 1,2-Diaminoanthraquinone for NO Gas Detection. *Macromol. Chem. Phys.* **2014**, *215*, 286−294.
(32) Chen, B.-Y.; Kuo, C.-C.; Huang, Y.-S.; Lu, S.-T.; Liang, F.-C.; Jiang, D.-H. Novel Highly Selective and Reversible Chemosensors Based on Dual-Ratiometric Fluorescent Electrospun Nanofibers with pH- and Fe3+-Modulated Multicolor Fluorescence Emission. *ACS Appl. Mater. Interfaces* **2015**, *7*, 2797−2808.
(33) Chen, L.-N.; Kuo, C.-C.; Chiu, Y.-C.; Chen, W.-C. Ultra metal ions and pH sensing characteristics of thermoresponsive luminescent electrospun nanofibers prepared from poly(HPBO-co-NIPAAm-co-SA). *RSC Adv.* **2014**, *4*, 45345−45353.
(34) Cho, C.-J.; Lu, S.-T.; Kuo, C.-C.; Liang, F.-C.; Chen, B.-Y.; Chu, C.-C. Pyrene or rhodamine derivative-modified surfaces of electrospun nanofibrous chemosensors for colorimetric and fluorescent determination of Cu 2+ , Hg 2+ , and pH. *React. Funct. Polym.* **2016**, *108*, 137−147.
(35) Hung, C.-C.; Kuo, C.-C.; Weng, N.-K.; Wu, W.-C.; Chen, B.-Y.; Cho, C.-J.; Hsu, I.-J.; Chiu, Y.-C.; Chen, W.-C. Novel highly sensitive and reversible electrospun nanofibrous chemosensor-filters composed of poly(HEMA-co-MNA) and bpy-F-bpy with metal-ion-modulated multicolor fluorescence emission. *Polym. J.* **2016**, *48*, 439−449.
(36) Li, L.; Yang, G.; Li, J.; Ding, S.; Zhou, S. Cell Behaviors on Magnetic Electrospun Poly-D, L-lactide Nanofibers. *Mater. Sci. Eng. C* **2014**, *34*, 252−261.
(37) Luo, L.; Cui, R.; Qiao, H.; Chen, K.; Fei, Y.; Li, D.; Pang, Z.; Liu, K.; Wei, Q. High Lithium Electroactivity of Electrospun CuFe2O4 Nanofibers as Anode Material for Lithium-Ion Batteries. *Electrochim. Acta* **2014**, *144*, 85−91.
(38) Min, M.; Wang, X.; Chen, Y.; Wang, L.; Huang, H.; Shi, J. Highly sensitive and selective Cu2+ sensor based on electrospun rhodamine dye doped poly(ether sulfones) nanofibers. *Sens. Actuators, B* **2013**, *188*, 360−366.
(39) Pelipenko, J.; Kocbek, P.; Kristl, J. Critical Attributes of Nanofibers: Preparation, Drug Loading, and Tissue Regeneration. *Int. J. Pharm.* **2015**, *484*, 57−74.

DOI: 10.1021/acsami.8b18366
ACS Appl. Mater. Interfaces 2019, 11, 10118−10127

(40) Zampetti, E.; Bearzotti, A.; Macagnano, A. Flexible Piezoelectric Transducer Based on Electrospun PVDF Nanofibers for Sensing Applications. *Procedia Eng.* **2014**, *87*, 1509−1512.
(41) Lin, C. C.; Jiang, D.-H.; Kuo, C.-C.; Cho, C.-J.; Tsai, Y.-H.; Satoh, T.; Su, C. Water-Resistant Efficient Stretchable Perovskite-Embedded Fiber Membranes for Light-Emitting Diodes. *ACS Appl. Mater. Interfaces* **2018**, *10*, 2210−2215.
(42) Wu, H.; Hu, L.; Rowell, M. W.; Kong, D.; Cha, J. J.; McDonough, J. R.; Zhu, J.; Yang, Y.; McGehee, M. D.; Cui, Y. Electrospun Metal Nanofiber Webs as High-Performance Transparent Electrode. *Nano Lett.* **2010**, *10*, 4242−4248.
(43) An, S.; Kim, Y. I.; Jo, H. S.; Kim, M.-W.; Lee, M. W.; Yarin, A. L.; Yoon, S. S. Silver-Decorated and Palladium-Coated Copper-Electroplated Fibers Derived From Electrospun Polymer Nanofibers. *Chem. Eng. J.* **2017**, *327*, 336−342.
(44) Ahn, Y.; Jeong, Y.; Lee, D.; Lee, Y. Copper Nanowire-Graphene Core-Shell Nanostructure for Highly Stable Transparent Conducting Electrodes. *ACS Nano* **2015**, *9*, 3125−3133.
(45) Chen, Z.; Ye, S.; Stewart, I. E.; Wiley, B. J. Copper Nanowire Networks with Transparent Oxide Shells that Prevent Oxidation without Reducing Transmittance. *ACS Nano* **2014**, *8*, 9673−9679.
(46) Hsu, P.-C.; Wu, H.; Carney, T. J.; McDowell, M. T.; Yang, Y.; Garnett, E. C.; Li, M.; Hu, L.; Cui, Y. Passivation Coating on Electrospun Copper Nanofibers for Stable Transparent Electrodes. *ACS Nano* **2012**, *6*, 5150−5156.
(47) Fischer, R.; Gregori, A.; Sahakalkan, S.; Hartmann, D.; Büchele, P.; Tedde, S. F.; Schmidt, O. Stable and highly conductive carbon nanotube enhanced PEDOT:PSS as transparent electrode for flexible electronics. *Org. Electron.* **2018**, *62*, 351−356.
(48) Lee, D.; Lee, H.; Ahn, Y.; Jeong, Y.; Lee, D.-Y.; Lee, Y. Highly stable and flexible silver nanowire-graphene hybrid transparent conducting electrodes for emerging optoelectronic devices. *Nanoscale* **2013**, *5*, 7750−7755.
(49) Tang, Y.; Ruan, H.; Huang, Z.; Shi, D.; Liu, H.; Chen, S.; Zhang, J. Fabrication of High-Quality Copper Nanowires Flexible Transparent Conductive Electrodes with Enhanced Mechanical and Chemical Stability. *Nanotechnology* **2018**, *29*, 455706.
(50) Ha, B.; Jo, S. Hybrid Ag Nanowire Transparent Conductive Electrodes with Randomly Oriented and Grid-Patterned Ag Nanowire Networks. *Sci. Rep.* **2017**, *7*, 11614.
(51) Lan, W.; Chen, Y.; Yang, Z.; Han, W.; Zhou, J.; Zhang, Y.; Wang, J.; Tang, G.; Wei, Y.; Dou, W.; Su, Q.; Xie, E. Ultraflexible Transparent Film Heater made of Ag Nanowire/PVA Composite for Rapid-Response Thermotherapy Pads. *ACS Appl. Mater. Interfaces* **2017**, *9*, 6644−6651.
(52) Lim, J.-E.; Lee, S.-M.; Kim, S.-S.; Kim, T.-W.; Koo, H.-W.; Kim, H.-K. J. S. r. Brush-Paintable and Highly Stretchable Ag Nanowire and PEDOT: PSS Hybrid Electrodes. *Sci. Rep.* **2017**, *7*, 14685.

DOI: 10.1021/acsami.8b18366
ACS Appl. Mater. Interfaces 2019, 11, 10118−10127